Grasp Quality Evaluation with Whole Arm Kinematic Noise Propagation

Shuo Liu Stefano Carpin

***Abstract*— In this paper we propose a new approach to evaluate grasps that accounts for both the kinematic structure of the robot and the noise at its joints. Our starting observation is that with a redundant robot the same grasp can be implemented with different arm configurations, and these may display significant differences in terms of robustness to disturbances. Consequently, the grasp quality metric is seen as a random variable depending on the arm configuration. Starting from a first order approximation for the error, we introduce the *high probability force closure region* as a tool to evaluate the local robustness of an arm configuration, and we then introduce a new metric Q_{arm} to rank different configurations according to the robustness to noise. By combining this method in an offline/online framework, we demonstrate through large scale simulations that this approach successfully captures aspects that were neglected in former literature regarding grasp evaluation, and can successfully be integrated into future grasp planners.**

I. Introduction

Grasp quality evaluation is strictly connected to grasp planning. Indeed, grasp quality is often used as an objective function to inform the search in the space of possible grasps. Two major areas of grasp quality metrics have been studied. The first one focuses on disturbance force rejection [7], [13], [23], [26], but does not consider the mechanical limitations of the robotic arm performing the grasp. For instance, the Ferrari-Canny metric [7] only considers the contact points without accounting for any kinematic constraint. Most of the methods in this group share a similar standpoint. The second area considers the hand structure and optimizes over certain aspects such as maximizing the smallest singular value of the hand Jacobian [25], the volume of the manipulability ellipsoid [32], or the maximum force applied at each contact [10]. Despite being at times overlooked, the mechanical structure of the hand is directly related to grasp quality since contacts are made between the hand and the target object. However, the arm is an equally important component in the system, but is seldom considered when evaluating grasp quality. Furthermore, many classical grasp quality metrics do not explicitly incorporate a noise-model, and therefore inaccuracies when a grasp is executed are not taken into account. This problem is extremely relevant for platforms with passive joints (e.g., Baxter [8]), where noise in joints is unavoidable.

S. Liu is with Amazon Robotics. S. Carpin is with the University of California, Merced, CA, USA.

This research was partially supported by NIST under cooperative agreement 70NANB12H143. Any opinions, findings, and conclusions or recommendations expressed in these materials are those of the authors and should not be interpreted as representing the official policies, either expressly or implied, of the funding agencies of the U.S. Government.

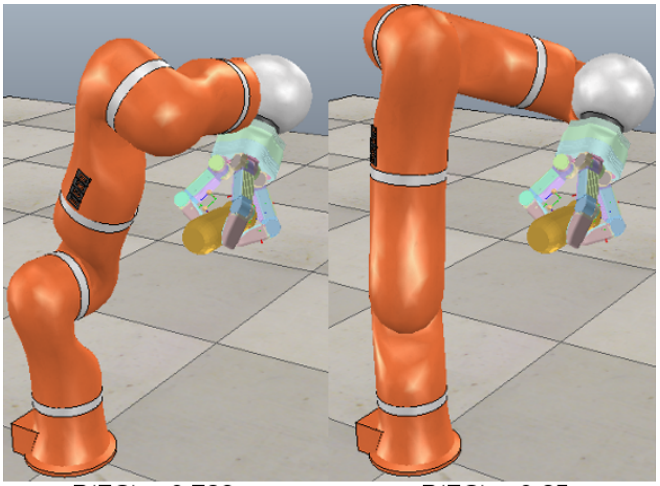

Fig. 1: Two grasps with identical contact points but different arm configurations. When identically distributed noise is applied to each joint, the corresponding probability of force closure $P(FC)$ is different.

In this work, we study the relationship between noise in the joints and the grasp quality metric defined by Ferrari and Canny (indicated as Q in the following). Noise is propagated by forward kinematics and the end-effector distribution is approximated using a first order expansion. Although the first order approximation does not provide an accurate bound, it still offers a rough distribution of the error distribution and provides a way to rank different arm configurations that can be used to achieve the same end-effector pose. According to this approach, the grasp quality measure Q is then a random variable and the ability to achieve a force closure grasp is an uncertain event. Therefore, we focus in on the probability of force closure measure $P(FC)$ [18] and the expected grasp quality $\mathbb{E}[Q]$ to evaluate the quality of a candidate grasp. Figure 1 illustrates the motivation for this work. It shows an example of two grasps with identical contacts at the finger tips, but different arm configurations. A classical analysis of these grasps not explicitly accounting for the different arm configurations and the associated noise would consider them perfectly equivalent. However, by superimposing to each joint a noise drawn from the same distributions, significant differences in terms of probability of force closure emerge. By generating 1000 samples in both cases, we experimentally assess that the one on the left has a significantly higher success probability. Accordingly, we argue that noise-modeling

should be accounted for to anticipate the probability of success of a candidate grasp. *The main goal of this work is to introduce a framework explicitly considering joint-level noise for grasp quality evaluation and synthesis.* The effect of uncertainties in mechanical structures has been extensively studied [6], but this is rarely considered in grasp evaluation and planning. This paper extends our previous study [16] by providing a method to quickly select the best arm configuration among all candidates. In particular, we propose a grasp quality metric that directly accounts for how joint-level noise impacts the probability of successfully completing a planned grasp.

The rest of this paper is organized as follows. Related work is discussed in Section II and in Section III we define the problem we consider and present the framework for our study. Experiments and their results are illustrated in Section IV and finally in Section V we summarize the lessons learned.

II. Background and Related Work

Analytic Grasp Synthesis

Because of its practical importance, grasp planning has been extensively investigated. Numerous grasp quality metrics have been proposed in the literature with the objective of solving the grasp synthesis problem using approaches based on optimization algorithms. The reader is referred to [2], [24] for a general introduction on grasping, including earlier physics-based models, such as the quasi-static model [20] to derive force or form closure grasps. The Ferrari-Canny metric [7] evaluates grasps based on the necessary effort to resist an arbitrary disturbance wrench in any direction acting on the object being grasped. This metric is by far the most well known and used, although it has certain drawbacks, i.e., it is not scale invariant, and it does not account for the geometry of the object. Strandberg and Wahlberg [26] improved this metric by only taking into account possible disturbance wrenches instead of arbitrary ones. The improved method is scale invariant and directly relates to the geometry of the object, but has been rarely used in practice due to its expensive computational cost. Liu and Carpin have recently developed two methods [14], [15] that notably expedite the computation process of these two metrics by using a paradigm based on partial convex hull computation. A comprehensive review of grasp quality metrics is presented in [25]. However, none of the methods discussed within the survey explicitly consider noise in the grasping process, and they are all based on physical models with known parameters, such as friction coefficients, contact points, and surface normals. In numerous practical applications, however, many of these parameters are only approximately known.

Data-Driven Approaches

Data-driven methods are an alternative approach to analytic grasp synthesis, whereby grasp configurations are obtained by learning from prior data. The reader is referred to [3], [12] for recent results in this growing area. For this type of methods noise is implicitly taken into account during data collection, but it is often not analytically modeled. Therefore, the ability to predict the effect in quality with respect to the noise in both the hand and the arm is limited and typically.

Noise modeling in mechanics

Noise modeling in mechanics has been well studied, e.g., in [22], where it is evidenced how noise in modeling robot arm mechanics is linked to numerous causes, like inaccuracies in the geometric models, backlash, nondeterministic errors due to friction, and quantization errors. Although many papers account for these noise sources through a linearized error propagation models and Gaussian distributions, papers such as [22] consider inaccuracies through error distributions empirically collected. Along with error modeling, a rich literature exists in parameter identification, using analytic approaches [9] or data-driven techniques [1], [27].

Noise modeling for grasping

Noise modeling for grasping has so far rarely been considered together with the kinematic structure. For example, [11] accounted for Gaussian errors in the end-effector positions, friction coefficient and object shape, and formulated the problem using a probabilistic framework. Similarly, Allen and collaborators [29] investigated uncertainty in the object model, which led to the notion of *probabilistic force closure*. Furthermore, [18] applied *probabilistic force closure* and introduced a cloud-based approach for sampling perturbations of grasps and leverage multi-armed bandits and deep learning to determine grasps with high probability of force closure. The approach we consider in this paper is instead focused on the impact of noise on the grasp quality metric, in particular through the whole-arm kinematic structure.

Inverse Kinematics

Inverse kinematics (IK) problems have been extensively studied in literature. For a manipulator with d joints it is defined as follows: given a pose $\mathbf{p} \in SE(3)$, compute a configuration $\mathbf{q} \in R^d$ such that by applying $\mathbf{q}$ to the manipulator, the end-effector pose is $\mathbf{p}$. If the joint number is smaller than six, the IK problem is in general not solvable for arbitrary poses, whereas if n is six, a unique solution can generally be obtained. When the number of joints is greater than six, redundancy is introduced, resulting in a solution space in which a specific configuration can then be selected based on one or more objectives (e.g., clearance from obstacles, used energy, etc.).

In the literature, IK problems are often solved using Jacobian based approaches and/or iterative methods. General solutions include pseudoinverse methods [30] and Jacobian transpose approaches [31]. However, these methods lack the ability to handle singularity problems. As an improvement to deal with these problems, the damped least square method was proposed in [21], [28]. In contrast to iterative methods, closed-form solutions can be computed by analytic approaches. The IKFast method, presented by Diankov in

[5], automatically determines a set of equations for closed-form IK solving. The algorithm performs well for solving IK problems with manipulators with up to six degrees of freedom. As an improvement, Diankov combined IKFast with a discretized sampling strategy in [4] to deal with redundancy. This method can then produce multiple solutions for a redundant manipulator with more than six joints.

III. Problem Definition and Methodology

Problem Definition

Consider a robot arm with d degrees of freedom equipped with a multifingered robotic hand, like the one shown in Figure 1. The forward kinematics (FK) function, $f : \mathbb{R}^d \rightarrow SE(3)$, maps a joint-configuration $\mathbf{q} = (q_1, \ldots, q_d) \in \mathbb{R}^d$ to the position and orientation of a frame rigidly attached to the end effector (e.g., to the center of the palm of the hand.) An approach widely used in grasp planning (see e.g. [19]) determines a pose of the reference point and then projects the contact points for the fingers assuming they are closed until contact is made with the object being grasped. Knowing the mechanical structure of the hand and of the object being grasped, this projection is a straightforward computation. Hence in the following we can treat $\mathbf{f} = f(\mathbf{q})$ as a grasp. The quality Q of the resulting grasp can then be calculated using one of the aforementioned metrics. In this work we assume the joint angles of the arm with d DOF are set to a desired target value $\mathbf{q_0}$ but superimposed noise exists at each joint. Specifically, noise is modeled as vector $\varepsilon = (\varepsilon_1, \ldots, \varepsilon_d)$, where the ε_is are independent random variables with a known distribution. For a realistic setup accounting for the mechanical limitations governing each joint, we consider each $|\varepsilon_i|$ to to be bounded by ε_{max}. Moreover, without loss of generality we assume each random component to have 0 mean. Distributions like the the truncated Gaussian[1] and the uniform distribution are obvious candidates to model this type of noise.

For the given setup, instead of reaching the target configuration $\mathbf{q_0}$, the arm will end up at $\mathbf{q} = \mathbf{q_0} + \varepsilon$. Consequently, the grasp quality Q is a random variable. We are therefore interested in the dependency between the random variable Q, the noise vector ε, and the kinematics of the robot arm. To be specific, for the grasp quality metric we consider the well known Ferrari-Canny metric that measures the size of the largest wrench along all directions that can be resisted by the grasp. For the case where the fingers fail to make contact with the object, or if the grasp does not achieve force closure, the value of the metric is undefined. To assess the effect of noise on Q, we consider the formerly mentioned probability of force closure $P(FC)$ and the expected quality metric $\mathbb{E}[Q]$. To study the properties of Q as a random variable, we consider different noise distributions and arm configurations achieving the same end-effector pose. The goal of our analysis is to identify variations in grasp robustness caused by variations in arm configurations, and reason about how we can computationally select the best arm configuration to achieve a higher $P(FC)$ for a target end-effector pose.

[1]This is a modified Gaussian distribution with 0 mean and whose density function is set to zero outside $[-\varepsilon_{max}, \varepsilon_{max}]$ and then normalized to integrate to 1. We use $\mathcal{N}(0, \sigma^2, \varepsilon_{max})$ to indicate this distribution.

A. Analytical approximation

As mentioned earlier, FK computes the pose of the end-effector as a function of the joint angles using the kinematic equations of a robot. For a given arm configuration $\mathbf{q_0}$, the corresponding end-effector pose can then be written as $\mathbf{f}_e = f(\mathbf{q_0})$. When noise is added in each joint, the end-effector pose is instead $\mathbf{f}'_e = f(\mathbf{q_0} + \varepsilon)$. The difference between the actual pose of the end effector and the desired pose can be written as

$$\Delta\mathbf{f}_e = f(\mathbf{q_0} + \varepsilon) - f(\mathbf{q_0}).$$

This mismatch is due to the error ε superimposed to the desired robot configuration $\mathbf{q_0}$. Let $\mathbf{J}$ be the Jacobian of the forward kinematics function f. For small values of ε, the error can be approximated as

$$\Delta\mathbf{f}_e \approx \mathbf{J}(\mathbf{q_0})\varepsilon.$$

According to our assumptions, each component of the disturbance vector satisfies the inequality $|\varepsilon_i| \leqslant \varepsilon_{max}$. If $\mathbf{q_0}$ is a non-singular configuration we can then write:

$$\Delta\mathbf{f}_e^T(\mathbf{J}\mathbf{J}^T)^{-1}\Delta\mathbf{f}_e \leqslant d||\varepsilon_{max}||_2^2$$

This inequality represents an ellipsoid for the error distribution of the end-effector pose with bounded noise ε. We dub this ellipsoid the *noise ellipsoid*. The length of the axes and the orientation of the noise ellipsoid are determined by the eigenvalues and eigenvectors of matrix $\mathbf{J}\mathbf{J}^T$. The noise ellipsoid is however accurate only for noise vectors ε with small norm, due to the first order approximation we used.

Although the approximation of the noise ellipsoid does not provide a tight bound, we can still use it to formulate the problem of computing an arm configuration to grasp an object that is robust to configuration disturbances. That is to say that among the various possible solutions provided by inverse kinematics in the case of a redundant manipulator, we can use robustness to noise as a selection criterion. To formalize the problem, we introduce the concept of *high probability force closure region* as follows.

Definition 1: Let $\mathbf{f}_e \in SE(3)$ be an end-effector pose that achieves a force closure grasp. The *high probability force closure region* associated to f_e with confidence ζ HPFCR($\mathbf{f}_e, \zeta$) is defined as the neighborhood of $\mathbf{f}_e$ such that

$$\forall \mathbf{f} \in \text{HPFCR}(\mathbf{f}_e, \zeta) \quad P_{FC}(\mathbf{f}) > \zeta$$

where $P_{FC}(\mathbf{f})$ is the probability that $\mathbf{f}$ achieves force closure.

Starting from this definition, we propose a sampling based approach to approximate the high probability for closure region. The steps are as follows.

1) Determine a force closure grasp with grasp quality value $Q_{\mathbf{f}_e} > Q_{MIN}$, where Q_{MIN} is a predetermined constant lower bound.

2) Given a bound b and step size s, sample the grasps around $\mathbf{f}_e$ within the cubical region with edge size $2b$ using step size s. Let P_{ALL} be the set of all such grasps.
3) Evaluate grasps in P_{ALL} and let $P \subset P_{ALL}$ the set of grasps that are force closure with quality larger than a threshold t_q.
4) Calculate the six-dimensional ellipsoid E fitting P with confidence percentage c. The confidence percentage refers to the percentage of points in set P that are within E. In the following we set $c = 70\%$, but the algorithm is not too sensitive to this value.
5) Compute $P(E)$, i.e., the probability of force closure of E as the ratio between the number of grasps in $E \cap P_{ALL}$ that are force closure and the total number of grasps in $E \cap P_{ALL}$. If $P(E) < \zeta$, increase t_q and go back to step 3. Otherwise, we terminate and set E to be HPFCR$(\mathbf{f}_e, \zeta)$.

Step 2 in the above procedure is the most critical because the end-effector pose is a six-dimensional vector and therefore brute force enumeration generates about $(\frac{2b}{s})^6$ grasps that must be evaluated. This problem is however mitigated in two different ways. First, this entire process is done offline in a precomputation step. Second, rather than enumerating all possible grasps in the regularly spaced grid, it is possible to rather generate just a subset of fixed size. Both these expedients are explained and illustrated in the following.

After obtaining the high probability force closure region, the next step is to use it to measure the quality of an arm configuration, i.e., the ability of an arm configuration to yield a grasp with high probability force closure despite joint-level noise. The following definition formalizes this idea.

Definition 2: Let $E = \text{HPFCR}(\mathbf{f}_e, \zeta)$ be the high probability force closure region for a grasp $\mathbf{f}_e$ and confidence ζ. By construction, E is a six-dimensional ellipsoid, and let $\mathbf{E}$ be the associated square matrix representing it. For a given arm configuration $\mathbf{q}_a$ such that $\mathbf{f}_e = f(\mathbf{q}_a)$, let $\mathbf{J}_a$ be the Jacobian matrix, and let $e_1, \ldots, e_6$ the eigenvalues of the matrix $d\varepsilon^2 \mathbf{E}^{-1}(\mathbf{J}_a \mathbf{J}_a^T)$. The grasp quality with respect to arm configuration $\mathbf{q}_a$ is

$$Q_{arm} = \frac{1}{\Sigma_i(\sqrt{e_i} - 1)^2}.$$

The rationale for this definition is as follows. $\sqrt{e_i}$ is the axis length of the ellipsoid determined by $d\varepsilon^2_{max}\mathbf{E}^{-1}(\mathbf{J}_a\mathbf{J}_a^T)$. Therefore $(\sqrt{e_i} - 1)^2$ measures the mismatch against the unit sphere along the $i-th$ dimension. Defined this way, Q_{arm} indicates how well the noise ellipsoid and the high probability force closure region are aligned, and higher values therefore represents more robustness to noise. Since for a given grasp, only $\mathbf{E}^{-1}$ is needed, we thereby store this information along with the grasp after the process of calculating the high probability force closure region.

The overall pipeline for our entire system is shown in Figure 2, and is divided into an offline and an online stage. For a given object, during the offline process, grasps with good quality are calculated along with their associated high probability force closure region. Each grasp is stored with its corresponding $\mathbf{E}^{-1}$ matrix in a database for online use. During the online process, the relative pose between the arm and the object to be grasped is determined, usually through by a vision pipeline as we did in [17]. Next, using IKFAST we obtain a set of candidate arm configurations, and determine which one to use after ranking them using the Q_{arm} metric we just introduced.

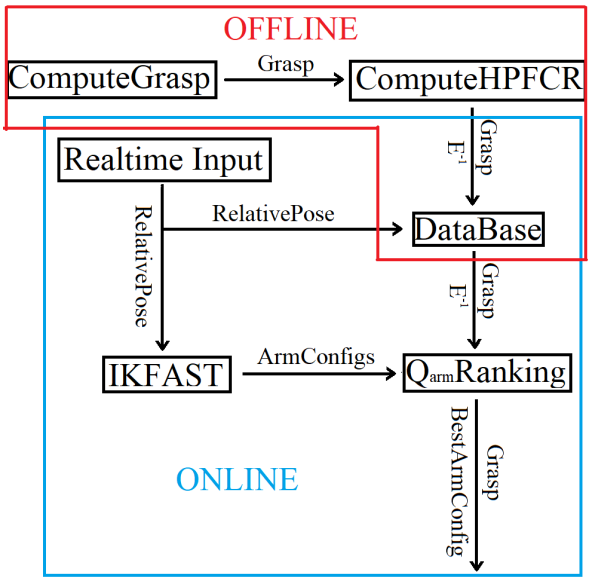

Fig. 2: The framework of our entire system.

Algorithm 1 sketches the online part of the algorithm. The input is the target grasp pose $\mathbf{p}_r$ and the matrix $\mathbf{E}^{-1}$ associated with the grasp. The output is the best arm configuration $\mathbf{q}_a$. The online part of the algorithm is efficient because it relies just on one call to IKFAST and several matrix multiplications.

Algorithm 1 Q_{arm} ranking algorithm

1: **Input** : $\mathbf{p}_r, \mathbf{E}^{-1}$
2: **Output**: Best arm configuration $\mathbf{q}_a$
3: $Q \leftarrow \text{IKFAST}(\mathbf{p}_r)$
4: **for all** $\mathbf{q}_j \in Q$ **do**
5: $\quad \mathbf{J}_j \leftarrow Jacobian(\mathbf{q}_j)$
6: $\quad e_i \leftarrow eigenvalues(d\varepsilon^2_{max}\mathbf{E}^{-1}(\mathbf{J}_j\mathbf{J}_j^T))$
7: $\quad Q_{arm_j} \leftarrow \frac{1}{\Sigma_i(\sqrt{e_i}-1)^2}$
8: $\mathbf{q}_a \leftarrow \{\mathbf{q}_j | j = \arg\max_j Q_{arm_j}\}$

IV. Experiments

We start by showing the limited mismatch between the noise ellipsoid and the actual end-effector pose distribution. Next, we present some examples of computation of the high probability force closure region. Finally, we use a sampling based aproximation of grasp quality for a 7-DOF Kuka Light weight robot arm (LWR) to show the performance of Q_{arm} metric.

A. Analytical based estimation of noise on end-effector pose

The noise ellipsoid produces an ellipsoid approximately aligned with the sampled end-effector distribution when a bounded noise is applied at each joint. Figure 3 shows the result of a simple experiment for a planar three-link arm. The noise applied to each joint is drawn from a uniform distribution with support $[-0.01, 0.01]$. The top subfigure shows the ratio between the eigenvalues defining the noise ellipsoid and the sampled end-effector position distribution with the same end-effector position. Over 1000 samples we can observe that ratio between the maximum and minimum eigenvalue remains close to 1. The bottom subfigure shows instead the 2-norm of the difference between the eigenvector matrices. The the small values indicate the substantial alignment between the noise ellipsoid and the sampled end-effector position, i.e., the fact that the approximation error introduced by the first order expansion is limited.

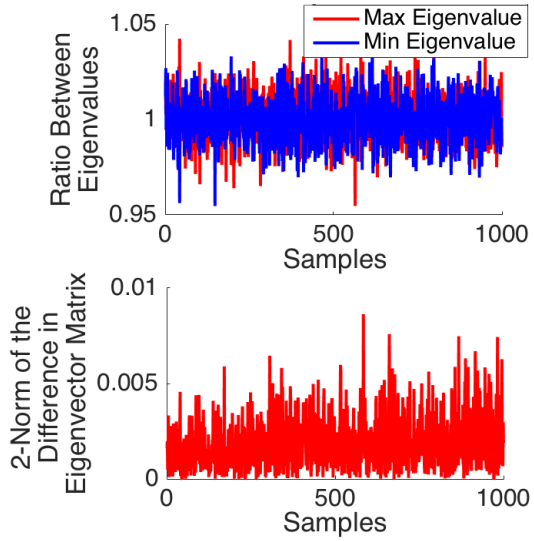

Fig. 3: The top subfigure shows the ratio between the eigenvalues of the noise ellipsoid and the sampled end-effector position distribution for a 3 link planar arm. The red line represents the ratio of maximum eigenvalue and the blue line represents the ratio of minimum eigenvalue. The bottom subfigure shows the 2-norm of the difference in the matrix representing all eigenvectors.

Similarly, figure 4 shows the comparison between the noise ellipsoid and the actual sampled end-effector distribution for a KUKA LWR arm. Data was gathered in simulation, thus allowing for flexibility in noise generation while relying on a high fidelity model for the arm. The noise applied at each of the seven joints is drawn from a uniform distribution with support $[-0.01, 0.01]$. The left subfigure shows the mean and variance of the scale between the eigenvalues, while the right subfigure shows the determinant of the difference in the matrix containing eigenvectors. Both figures confirm that the error is small.

Finally, Figure 5 contrasts the sampled end-effector position distribution, when noise drawn from a uniform distribution with support $[-0.01, 0.01]$ is applied to all joints. For each shown configuration, 10,000 samples were generated to determine the distribution of the end-effector position. The figure confirms that the sampled end-effector distribution is well aligned with the noise ellipsoid. For the 7 DOF KUKA arm, the noise ellipsoid therefore provides a good indication of the actual sampled noise distribution.

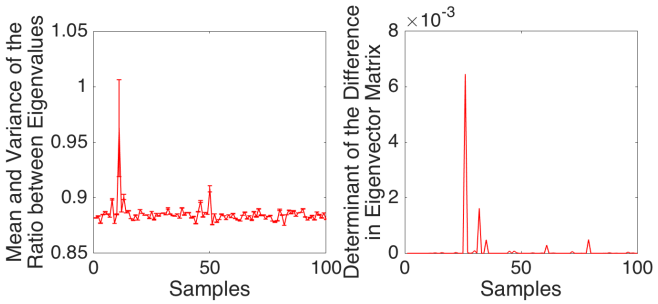

Fig. 4: The left subfigure shows the mean and variance of the scale between the eigenvalues of the noise ellipsoid and the sampled end-effector position distribution for KUKA LWR. The right subfigure shows the determinant value of the difference in the matrix representing all eigenvectors.

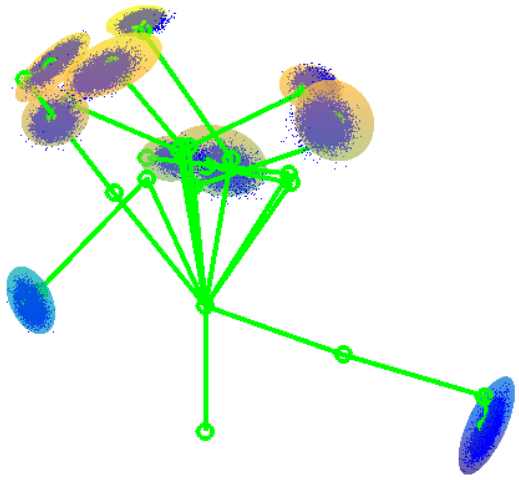

Fig. 5: Sampled end-effector position distribution with noise shown in blue and noise ellipsoid for a 7 DOF KUKA arm (shown in colored ellipsoid).

B. High Probability Force Closure Region

Our grasp quality measure Q_{arm} relies on the high probability force closure region. Figure 6 shows an SDH hand grasping a bottle (this study is instead done using the VREP simulator), whereas Figure 7 shows the corresponding high probability force closure region projected in the position domain and the orientation domain. All points shown as either red dots or blue dots represent force closure grasps, but red dots are the points within ellipsoid associated to the high probability force closure region. To be more specific, the high probability force closure region is sampled around the grasp with the bound $b = 0.03$ and step size $s = 0.06$. The

confidence percentage c was set to 70% to filter out points too far away from the center of the ellipsoid E. The quality threshold was select with $t_q = 0.2144$, which is equal to half of the maximum quality value over all samples. This value is selected to achieve a force closure probability of more than 50% within the high probability force closure region. As shown in figure 7, the ellipsoid in the orientation domain is comparably larger than the ellipsoid in the position domain. Blue dots in the left figure are not evenly distributed, as can be observed noting the lack of points in the left part. This observation confirms that the high probability force closure region is biased towards good grasps, so choosing the associated arm configuration will benefit the final outcome.

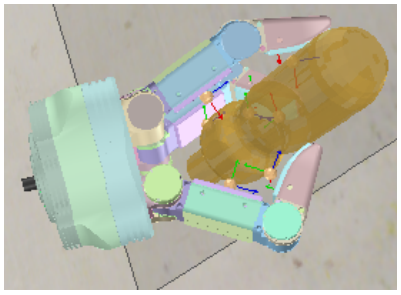

Fig. 6: Example grasp on a bottle object.

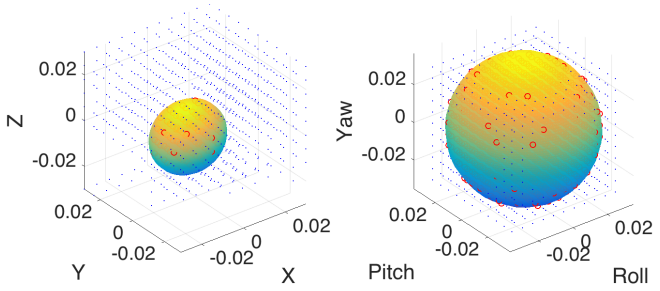

Fig. 7: The High Probability Force Closure Region projected in XYZ-coordinate system (left) and RPY-coordinate system (right).

Figure 8 shows the relationship between the force closure probability and the volume of the ellipsoid E with respect to the quality threshold t_q. t_q is sampled from 10% of the maximum quality up to 90% of the maximum quality (that in this specific case is 0.4288). As t_q increases, the force closure probability also increases whereas the volume of E shrinks as expected. The ideal probability force closure region would be the largest region enclosing the probability threshold. Thus, our iterative method that increases t_q at each iteration is sufficient to locate the ideal probability force closure region.

To accelerate the speed to compute the high probably force closure region, we can first investigate the variance of the end-effector distribution in both the position and orientation domains. For example, the end-effector distribution of the KUKA LWR arm distribution varies more in the position domain compared to the orientation domain. Therefore, we can decrease the size of the bound b for the orientation domain to improve the efficiency of the algorithm.

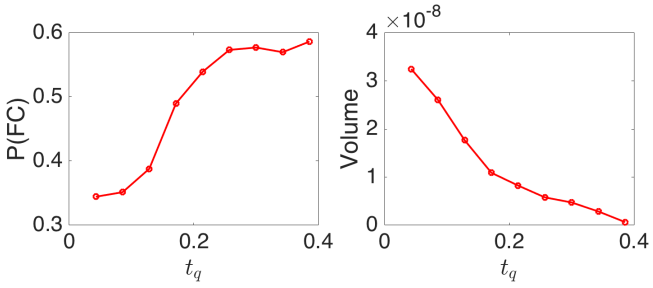

Fig. 8: Trend of force closure probability (left) and volume of fitting ellipsoid (right) with respect to t_q.

C. Validation in Simulation

To perform an end-to-end validation of our method in simulation, we generate the end-effector noise distribution by applying noise drawn from a truncated Gaussian distribution at each joint and for each end-effector pose we compute the corresponding grasp quality. In particular, we compare the the best arm configuration and the worst arm configuration selected by Q_{arm} optimizing $P(FC)$ as defined before and $\mathbb{E}[Q]$ defined as the expected force closure quality among all force closure grasps. Figure 9 shows the comparison between the best arm configuration (in red) and the worse arm configuration (in blue) for two different objects under different noise. The $P(FC)$ and $\mathbb{E}[Q]$ values of the best configuration for both objects are in average higher than the value for the worst arm configuration, especially when the noise is large. The high probability force closure region is computed by sampling within a certain range. For a relatively small noise, most arm configurations might be included inside the high probability force closure region, therefore the $P(FC)$ shows less change among all arm configurations. The difference is more significant when the noise is large, such that a more aligned noise distribution against the high probability force closure region has a higher chance to be force closure. Similar results were obtained for other objects.

V. Conclusions

In this paper, we proposed a framework to analytically address the inter-relation between grasp quality evaluation functions, joint-level noise, and the mechanical structure of the robotic arm. In our previous research, we showed the effect and importance of taking the arm configuration into account while evaluating grasp quality. As an extension, this work proposes two important concepts, i.e., the high probability force closure region, and a new grasp quality metric Q_{arm} to explicitly consider the structure of the arm and disturbances when evaluating different ways to implement a target grasp. This metric can be integrated with existing grasp quality measures to quantify the quality of the entire robotic system.

The method we use is based on the first order approximation of the forward kinematics, but our experiments shows that this is sufficient to obtain significant gain in robustness of the grasp by ranking the arm configurations

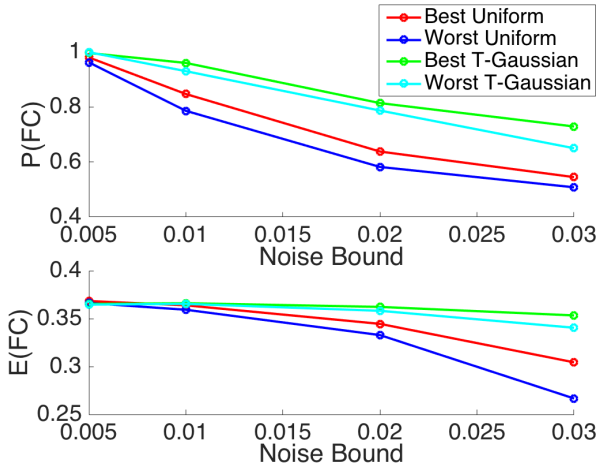

Fig. 9: $P(FC)$ and $\mathbb{E}[Q]$ for object bottle under difference noise distribution with different noise. For each value ε for the noise bound, the superimposed noise is a truncated Gaussian $\mathcal{N}(0, (\frac{\varepsilon}{3})^2, \varepsilon)$.

using Q_{arm}. Although the offline algorithm determining the high probability force closure region is time consuming, our method is efficient for online use.

In this paper we have mostly focused on the noise acting on the robot joints and how to select the most suitable arm configuration to gain the success rate of a grasp or its quality. One could argue that noise may be negligible for many robots, but with the current trend of relying more and more on inexpensive robots, it appears that this aspect will be extremely important in the future.

REFERENCES

[1] P.R. Barragan, L.P. Kaelbling, and T. Lozano-Perez. Interactive bayesian identification of kinematic mechanisms. In *Proceedings of the IEEE International Conferene on Robotics and Automation*, pages 2013–2020, 2014.

[2] A. Bicchi and V. Kumar. Robotic grasping and contact: A review. In *Proceeding of the IEEE International Conference on Robotics and Automation*, pages 348–353, 2000.

[3] J. Bohg, A. Morales, T. Asfour, and D. Kragic. Data-driven grasp synthesis—a survey. *IEEE Transactions on Robotics*, 30(2):289–309, 2014.

[4] R. Diankov. *Automated construction of robotic manipulation programs*. PhD thesis, Carnegie Mellon University, 2010.

[5] R. Diankov and J. Kuffner. Openrave: A planning architecture for autonomous robotics. *Robotics Institute, Pittsburgh, PA, Tech. Rep. CMU-RI-TR-08-34*, 79, 2008.

[6] D. Dornfeld and M.M. Halu. *Precision Manufacturing*. Springer, 2008.

[7] C. Ferrari and J. Canny. Planning optimal grasps. In *Proceedings of the IEEE International Conference on Robotics and Automation*, pages 2290–2295. 1992.

[8] E. Guizzo and E. Ackerman. How rethink robotics built its new baxter robot worker. *IEEE Spectrum*, 2012.

[9] R. He, Y. Zhao, S. Yang, and S. Yang. Kinematic-parameter identification for serial-robot calibration based on poe formula. *IEEE Transactions on Robotics*, 26(3):411–423, 2010.

[10] R. Krug, Y. Bekirogluz, and M. A. Roa. Grasp quality evaluation done right: How assumed contact force bounds affect wrench-based quality metrics. In *Proceedings of the IEEE International Conference on Robotics and Automation*, 2017.

[11] M. Laskey, J. Mahler, Z. McCarthy, F.T. Pokorny, S. Patil, J. van den Berg, D. Kragic, P. Abbeel, and K. Goldberg. Multi-armed bandit models for 2d grasp planning with uncertainty. In *Proceedings of the IEEE International Conference on Automation Science and Engineering*, pages 572–579, 2015.

[12] S. Levine, P. Pastor, A. Krizhevsky, and D. Quillen. Learning hand-eye coordination for robotic grasping with deep learning and large-scale data collection. *arXiv preprint arXiv:1603.02199*, 2016.

[13] Z. Li and S S. Sastry. Task-oriented optimal grasping by multifingered robot hands. *IEEE Journal of Robotics and Automation*, 4(1):32–44, 1988.

[14] S. Liu and S. Carpin. A fast algorithm for grasp quality evaluation using the object wrench space. In *Proceedings of the IEEE Conference on Automation Science and Engineering*, pages 558–563, 2015.

[15] S. Liu and S. Carpin. Fast grasp quality evaluation with partial convex hull computation. In *Proceedings of the IEEE International Conference on Robotics and Automation*, pages 4279–4285, 2015.

[16] S. Liu and S. Carpin. Kinematic noise propagation and grasp quality evaluation. In *Proceedings of the IEEE Conference on Automation Science and Engineering*, pages 1177–1183, 2016.

[17] S. Liu, Z. Hu, H. Zhang, M. Kwon, Z. Wang, Y. Xu, and S. Carpin. Grasp quality evaluation and planning for objects with negative curvature. In *Proceedings of the IEEE International Conference on Robotics and Automation*, pages 2223–2229, 2017.

[18] J. Mahler, F. T Pokorny, B. Hou, M. Roderick, M. Laskey, M. Aubry, K. Kohlhoff, T. Kröger, J. Kuffner, and K. Goldberg. Dex-net 1.0: A cloud-based network of 3d objects for robust grasp planning using a multi-armed bandit model with correlated rewards. In *Proceedings of the IEEE International Conference on Robotics and Automation*, pages 1957–1964, 2016.

[19] A.T. Miller and P.K. Allen. Graspit! a versatile simulator for robotic grasping. *IEEE Robotics Aut. Mag.*, 11(4):110–122, 2004.

[20] Richard M Murray, Zexiang Li, S Shankar Sastry, and S Shankara Sastry. *A mathematical introduction to robotic manipulation*. CRC press, 1994.

[21] Y. Nakamura and H. Hanafusa. Inverse kinematic solutions with singularity robustness for robot manipulator control. *ASME, Transactions, Journal of Dynamic Systems, Measurement, and Control*, 108:163–171, 1986.

[22] D.S. Necsulescu, A. Fahim, and C. Lu. Stochastic error propagation in robot arms. *Advanced Robotics*, 8(5):459–476, 1994.

[23] N. S Pollard. Parallel methods for synthesizing whole-hand grasps from generalized prototypes. Technical report, DTIC Document, 1994.

[24] D. Pratticchizzo and J.C. Trinkle. Grasping. In B. Siciliano and O. Khatib, editors, *Handbook of robotics*, chapter 28, pages 671–700. Springer, 2008.

[25] M. A Roa and R. Suárez. Grasp quality measures: review and performance. *Autonomous Robots*, 38(1):65–88, 2015.

[26] M. Strandberg and B. Wahlberg. A method for grasp evaluation based on disturbance force rejection. *IEEE Transactions on Robotics*, 22(3):461–469, 2006.

[27] J. Sturm, C. Stachniss, and W. Burgard. A probabilistic framework for learning kinematic models of articulated objects. *Journal of Artificial Intelligence Research*, pages 477–526, 2011.

[28] C. W Wampler. Manipulator inverse kinematic solutions based on vector formulations and damped least-squares methods. *IEEE Transactions on Systems, Man, and Cybernetics*, 16(1):93–101, 1986.

[29] J. Weisz and P.K. Allen. Pose error robust grasping from contact wrench space metrics. In *Proceedeings of the IEEE International Conference on Robotics and Automation*, pages 557 – 562, 2012.

[30] D. E Whitney. Resolved motion rate control of manipulators and human prostheses. *IEEE Transactions on man-machine systems*, 10(2):47–53, 1969.

[31] W. Wolovich and H. Elliot. A computational technique for inverse kinematics. In *Proceedings of The 23rd IEEE Conference on Decision and Control*, pages 1359–1363, Dec. 1984.

[32] T. Yoshikawa. Manipulability of robotic mechanisms. *The international journal of Robotics Research*, 4(2):3–9, 1985.